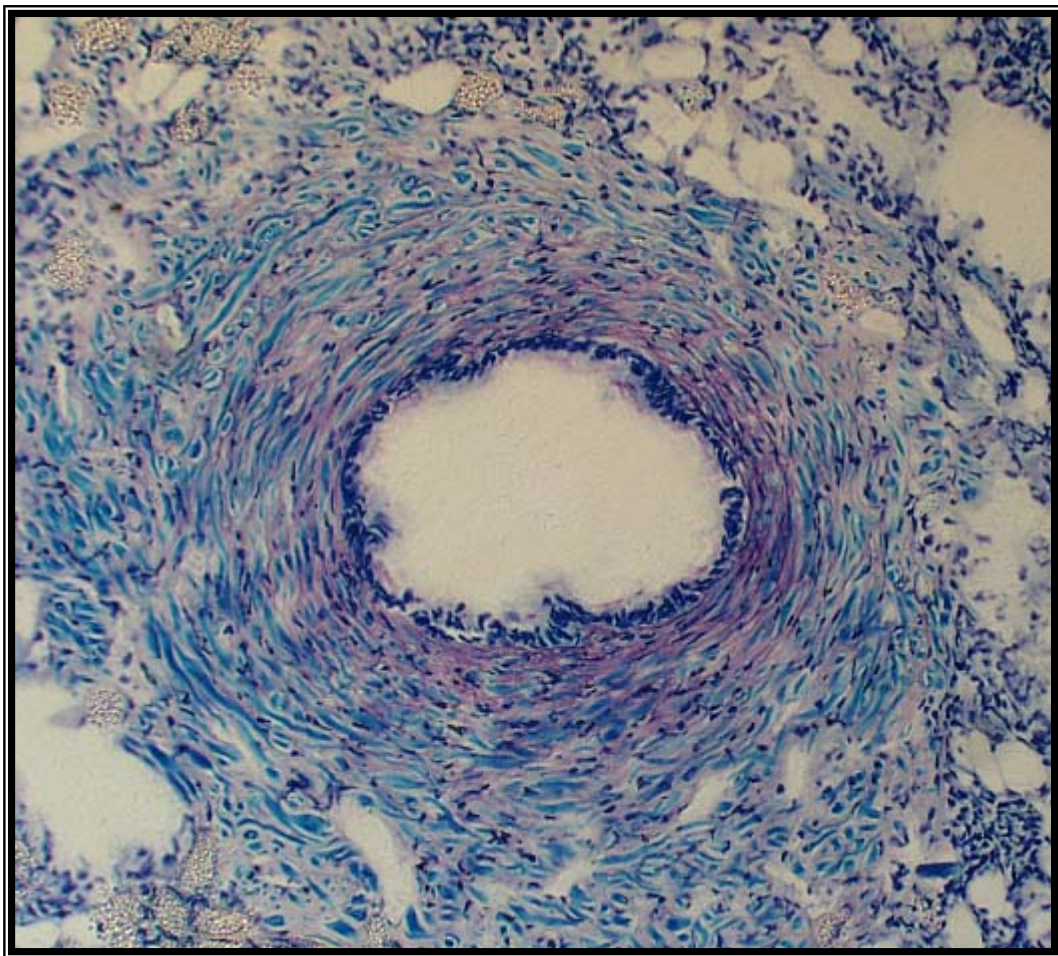


Chapter 3

Histomorphology of the pallial gonoduct, hypobranchial gland and associated structures in *Dicathais orbita* (Neogastropoda: Muricidae)



Publication of chapter subset

WESTLEY, C., LEWIS, M. C. and BENKENDORFF, K. Histomorphology of the female pallial gonoduct in *Dicathais orbita* (Neogastropoda: Muricidae): Sperm passage, fertilization and sperm storage potential. *Inverteb. Biol.* Accepted 20th February 2009.

3.0 Abstract

Bioactive Tyrian purple precursors occur in the hypobranchial gland, reproductive glands and egg masses of muricids such as *Dicathais orbita*. Histomorphological examination was conducted over the annual cycle to gain a detailed understanding of these structures in *D. orbita* and to determine a mechanism for precursor transfer from the hypobranchial gland to the pallial gonoduct. Gonoduct anatomy, musculature and spermatozoa distribution allowed the process of fertilization to be proposed for the first time in *D. orbita*. The temporal approach of this investigation revealed morphological plasticity in the gonoduct of this species and a potential capacity for long-term sperm storage and ingestion. The taxonomic and ecological implications of these findings are discussed. Seven secretory cell types were identified in the hypobranchial epithelium of *D. orbita*, which can be broadly classified into cells which secrete mucoproteins and acidic sulphated mucopolysaccharides. Three secretory cells new to the Muricidae were identified, along with two cell types which appear to be associated with Tyrian purple synthesis. A vascular sinus containing the rectum and rectal gland occurs in the subepithelial space between the hypobranchial gland and pallial gonoduct. Examination of this region failed to reveal an anatomical connection for precursor transfer. This, coupled with similarities in the properties of hypobranchial, capsule and albumen gland secretions suggests that the prochromogen is synthesized in the pallial gonoduct before incorporation into egg masses.

3.1 Introduction

Muricid molluscs, along with all caenogastropods, have internal fertilization and deposit their eggs within capsules. This mode of reproduction is facilitated by a suite of specialized glandular structures, which have long been considered of diagnostic value for cladistic analyses (Middelfart, 1992a, b, 1993; Kool, 1993; Lindberg and Ponder, 2001; Tan, 2003). The female albumen gland secretes perivitelline fluid around the eggs before they are transferred to the capsule gland where the egg capsule is elaborated. The capsule is then passed onto the ventral pedal gland for hardening and attachment to the substrate (Fretter, 1941). A bursa copulatrix may also be present, which receives sperm before they enter a sac-like organ or a series of ducts adjoining the albumen gland, called seminal receptacles. Sperm are thought to be stored and maintained here until required for fertilization (Ramorino, 1975; Jaramillo, 1991). Females may also possess an ingesting gland, which functions in the digestion of surplus gametes (Fretter, 1941).

Key morphological features of the bursa copulatrix, seminal receptacles, capsule, ingesting and albumen glands have been documented for many Muricidae (Kool, 1993; Middelfart, 1993; Tan, 2003), and examined extensively in *Ocenebra erinacea*, *Nucella (Purpura) lapillus* (Fretter 1941), *Concholepas concholepas* (Ramorino, 1975), *Plicopurpura patula* (Kool, 1988), *Chorus giganteus* (Jaramillo, 1991), *Chicoreus brunneus* (Middelfart, 1992a), *C. ramosus* (Middelfart, 1992b; Aungtonya, 1997), and *C. capucinus* (Aungtonya, 1997). The hypobranchial gland, renowned for production of the ancient dye Tyrian purple, is also of some taxonomic importance (Kool, 1993; Tan, 2003). Detailed accounts have been published for *N.*

lapillus (Letellier, 1890; Bernard, 1890), *Murex brandaris* (Bolognani-Fantin and Ottaviani, 1981), *Morula granulata* (Srilakshmi, 1991), *Thais haemastoma canaliculata* (Roller et al., 1995) and, *Plicopurpura pansa* (Naegel and Aguilar-Cruz, 2006). Previous investigations have dealt with the pallial gonoduct and hypobranchial gland separately; however recent evidence suggests an anatomical connection may exist between these glandular structures (Benkendorff et al., 2004; Westley and Benkendorff, 2008).

Tyrian purple is synthesized in the hypobranchial gland of muricid molluscs from the prochromogen, tyrindoxyl sulphate (Baker and Sutherland, 1968). By action of an arylsulphatase enzyme, intermediates are generated, and in the presence of sunlight, Tyrian purple evolves (reviewed in Cooksey, 2001a). Tyrian purple genesis also occurs in muricid egg masses (Palma et al., 1991; Benkendorff et al., 2000, 2001, 2004), which has prompted investigation into a possible reproductive role (Westley et al., 2006). Observations of purple pigmentation in the reproductive glands of *D. orbita* (Benkendorff et al., 2004) imply that Tyrian purple precursors may be incorporated into muricid egg masses from a maternal source. Recently, the potential for precursor transfer from the adult gonoduct to the egg masses during encapsulation has been supported by detection of the prochromogen in albumen and ingesting glands, and additionally, bioactive intermediate precursors in the capsule gland (Westley and Benkendorff, 2008). The capsule gland presents a possible location for the incorporation of both precursors and biosynthetic enzymes from the adjacent hypobranchial gland during capsule formation (Westley and Benkendorff, 2008). Similarly, the albumen gland may facilitate inclusion of the prochromogen into albuminous secretions (Westley and Benkendorff, 2008). Overall, the presence of

hypobranchial gland metabolites in muricid egg capsules (Palma et al., 1991; Benkendorff et al., 2000, 2001, 2004) and the pallial gonoduct of *D. orbita* (Benkendorff et al., 2004; Westley and Benkendorff, 2008), suggests the potential for maternal investment in embryonic chemical defence. Consequently, we aim to present the first detailed description of the pallial gonoduct and hypobranchial gland of *D. orbita* with the intention of deciphering an anatomical connection for precursor transfer.

3.2 Methods and materials

D. orbita specimens were sampled from subtidal rocky platforms along the Fleurieu Peninsula of South Australia. As hypobranchial gland secretory activity is thought to elevate during the breeding season (Fretter and Graham, 1994), mechanisms of precursor transfer may become more apparent during the copulating or egg-laying seasons. Consequently, triplicate females representing each of four reproductive phases were collected to allow comparisons of gross morphological and histochemical features over the annual cycle; 1) copulating females were gathered from large aggregations of males and females during late August, 2005; 2) laying females were taken directly from egg masses and sampled repeatedly from November to December, 2005 in the hope of observing capsule formation; 3) post- and; 4) pre-reproductive females were obtained in March and early July, 2006, respectively. Sex was determined by the presence of albumen, ingesting and capsule glands, and the absence of a penis.

The shell of each live specimen was measured from spire to siphonal canal (0.01mm) with vernire calipers. The shell was then removed by cracking with a vice

at the junction of the primary body whorl and spire, and the soft body removed by severing the columnar muscle. The soft body was then transferred to a dissecting tray and submersed in filtered (0.22 μ m) seawater to reduce osmotic stress. The dorsal mantle and pallial gonoduct were separated from the rest of the visceral mass by an incision along the lateral margins of the columnar muscle. For gross morphological descriptions, digital images of the dorsal mantle were taken under a stereo-dissecting microscope (Olympus, SZH). The mantle was then folded back and pinned with the ventral surface facing up. Images of the hypobranchial gland epithelium, capsule, ingesting and albumen glands and seminal receptacles were then acquired. Ingesting and capsule gland, length and radius, were also determined with an eyepiece micrometer (0.01mm) to permit calculation of glandular volumes (based on a cylinder). Measurements of shell length were employed for volume normalization.

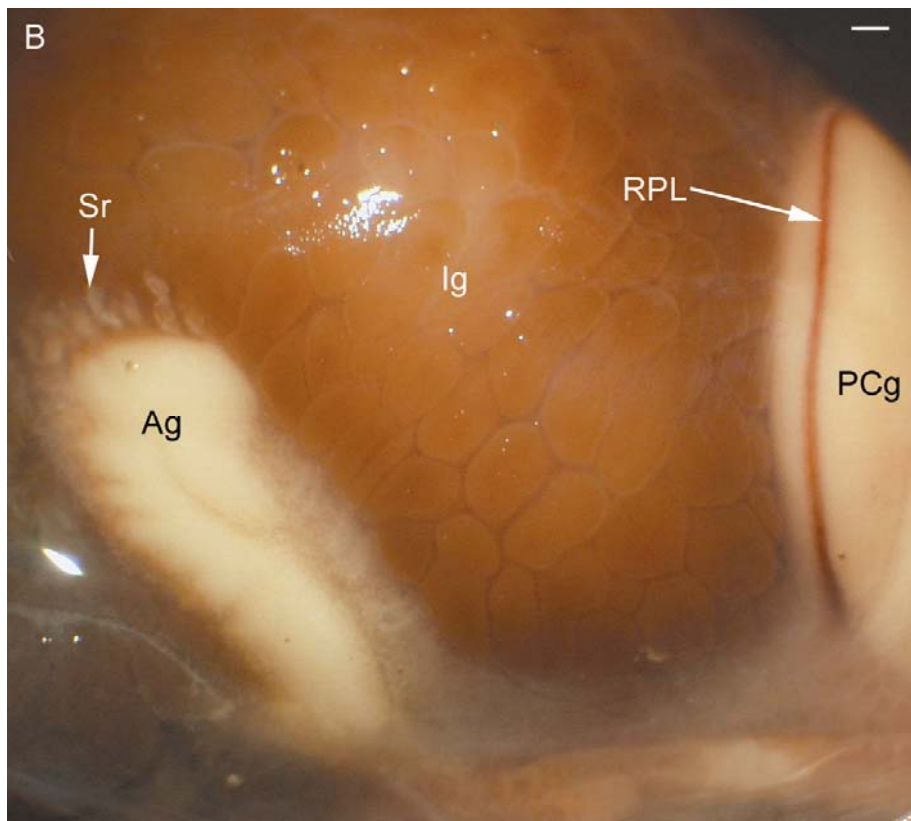
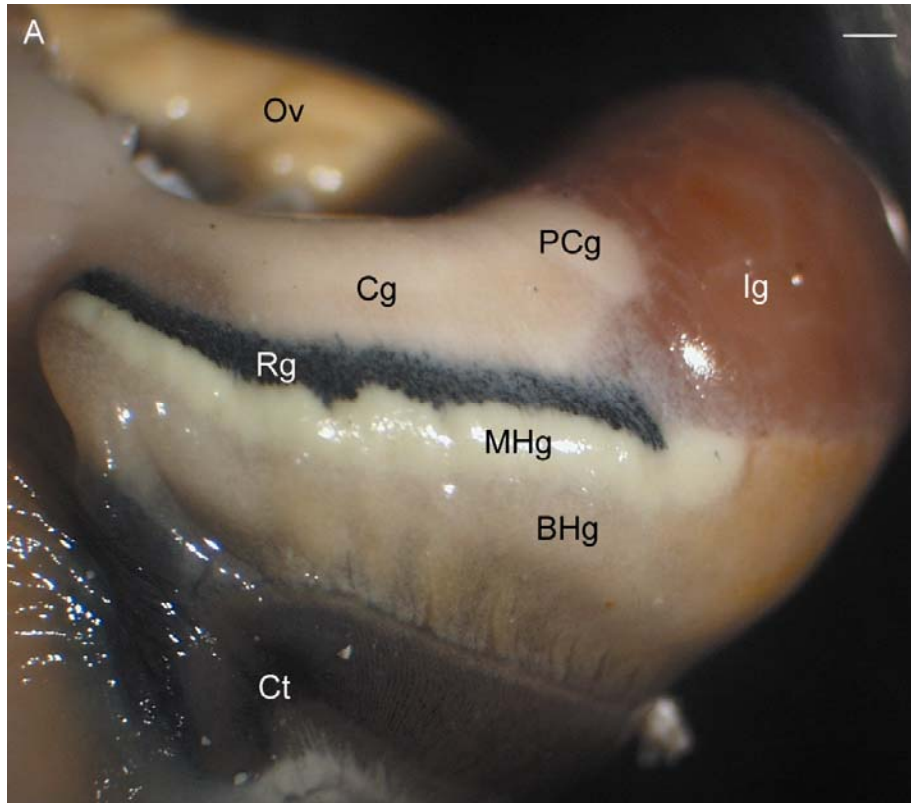
Longitudinal and transverse incisions were made along the junction between the ctenidium and branchial hypobranchial epithelium, and the ingesting and digestive glands, respectively. The pallial gonoduct of each specimen, complete with dorsal mantle and hypobranchial gland, was then fixed in 10% neutral buffered formalin for 6hrs, dehydrated through an ethanol series, cleared in chloroform and embedded in paraffin. A minimum of 18 serial transverse sections (5 μ m) were obtained from five regions of interest for all 12 specimens. These regions included the anterior pallial gonoduct, medial capsule gland, posterior capsule gland, anterior ingesting gland and the posterior ingesting gland, which also contains the albumen gland and seminal receptacles. Six serial sections from each region were stained with; 1) Modified Harris Haematoxylin and Eosin Y with Phloxine B (Thompson, 1966) or Lillie-Mayer's Haematoxylin and Eosin (Lillie, 1977) for routine histological

description, 2) Periodic Acid Schiff (McManus, 1946) for the demonstration of mucous cells, and 3) Toluidine Blue (Kramer and Windrum, 1954) for the differentiation of neutral (Wägele et al., 2006), sulphated-acid (Kramer and Windrum, 1954) and phenol-acid mucopolysaccharides (Ramalingam and Ravindranath, 1970). Sections were examined under a compound light microscope (Olympus, BH-2) and measurements of hypobranchial gland cells were obtained with an eyepiece micrometer (0.01 μ m) from epithelial regions prominent for each cell type.

3.3 Results

3.3.0 Gross morphology

The ventral dorsal mantle of *D. orbita* is characterized by an anteroposteriorly elongated hypobranchial gland, which extends from a left lateral ctenidium (Fig. 1a) to surround the ventral surface of the rectum on the right. The rectum is embedded in the left lateral portion of the pallial gonoduct, which occupies the right mantle cavity. From anterior to posterior, the gonoduct is comprised of a capsule, ingesting and albumen gland (Fig.1a-c). A prominent rectal gland runs dorsal to the capsule gland (Fig. 1a, 1c).



C

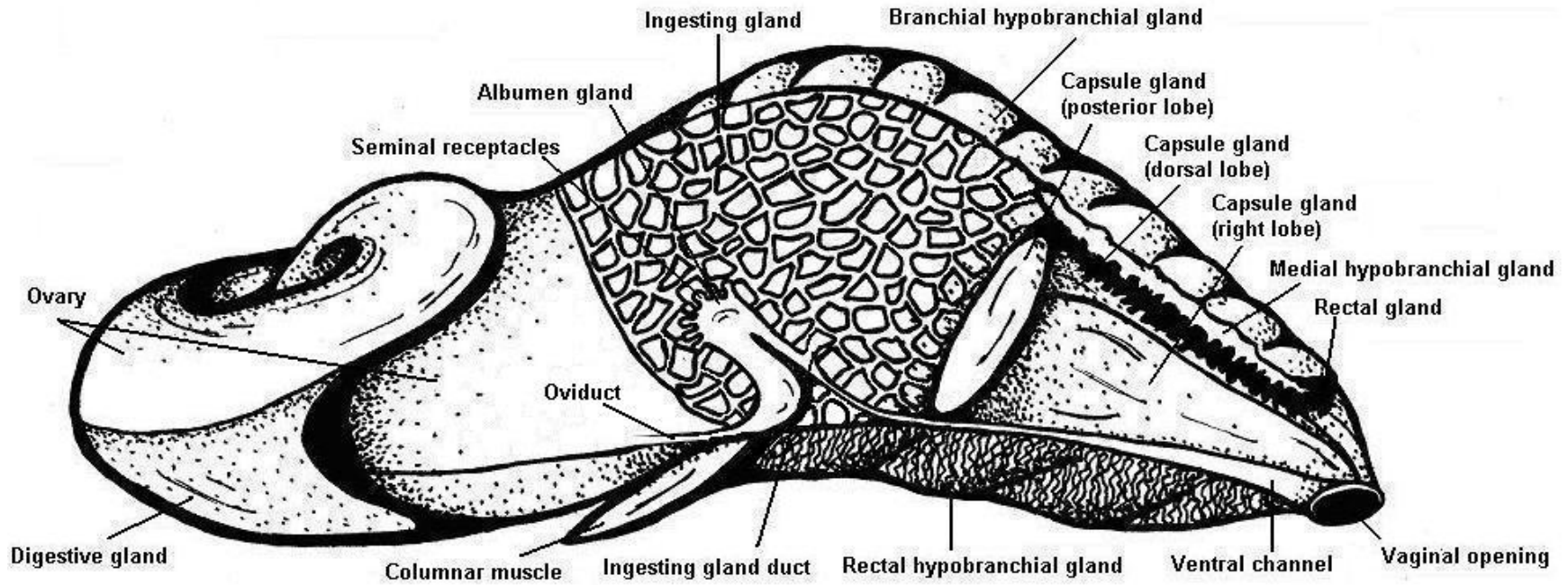


Figure 1. The pallial gonoduct and hypobranchial gland of an egg-laying female *D. orbita*. (A) Dorsal view of the anterior pallial gonoduct showing the yellow ovary (Ov), capsule gland (Cg), posterior capsule gland lobe (PCg), rectal gland (Rg), ingesting gland (Ig), medial hypobranchial gland (MHg), branchial hypobranchial gland (BHg), and ctenidium (Ct); (B) right side of the posterior pallial gonoduct showing the red pigmented line (RPL) on the posterior capsule gland lobe, the multiple chambers of the ingesting gland (Ig), and the albumen gland (Ag), complete with dorsal and posterior seminal receptacles (Sr); and (C) a hand drawn schematic detailing the anatomical connections between these glandular features. Scale bars = 1mm. Schematic is not to scale.

The hypobranchial gland is divided into three well defined sections, a left lateral branchial region, an adjacent medial region, and a right lateral rectal region (Fig. 2). The lateral regions extend posteriorly for the length of the pallial gonoduct and the epithelium is composed of transverse folds, orientated perpendicular to the mantle. The medial region exists as a slight depression between the branchial and rectal regions, and can be seen through the dorsal integument, to commence and terminate with the capsule and rectal gland (Fig. 1a, 1c). The medial region was invariably covered in a viscous, cream coloured secretion (Fig. 2), which consecutively gained yellow, red, green and finally purple pigmentation, along with a pungent sulphurous odour, after exposure to oxygen and light. Although the lateral regions were devoid of secretion, epithelial pigmentation was consistently orange in reproductively active females (Fig. 2) and cream during the remainder of the year.

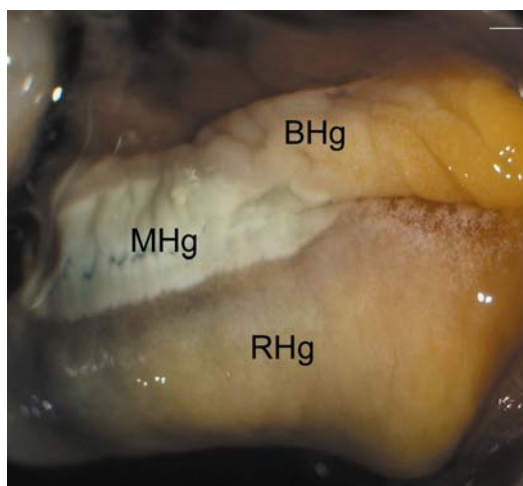


Figure 2. The ventral surface of the mantle displaying the orange pigmented branchial (BHg) and rectal (RHg) regions of the hypobranchial gland in an egg-laying female, and the medial depression (MHg), covered in cream mucous, which turns purple after exposure to sunlight. Scale bar = 1mm

Ventral to the anus, a partially detached muscular extension of the anteroposteriorly elongated capsule gland contains the vaginal opening. The capsule gland is a white glandular mass, composed of two lateral lobes, a dorsal lobe and a prominent posterior lobe, which develops a dorsoventral line of red pigmentation during the reproductive season (Fig. 1b). The ingesting gland is located posterior to the capsule gland, and appears as a pigmented glandular structure with numerous chambers (Fig. 1b). A laterally compressed, staff-shaped albumen gland is partially embedded in the posteroventral portion of the ingesting gland on its right lateral side (Fig. 1b, 1c). Numerous seminal receptacles (7-8) are discernable through the integument along the dorsal and posterior periphery (Fig. 1b, 1c). The albumen gland and seminal receptacles are typically white, but gain orange pigmentation in a post-reproductive state (Fig. 3).

The capsule and ingesting glands displayed considerable morphological plasticity over the course of the annual cycle. Pre-copulation, the capsule gland becomes enlarged ($16.01 \pm 10.49\text{mm}^3$), while the ingesting gland is comparatively reduced ($9.19 \pm 5.89\text{mm}^3$) and devoid of pigmentation (Fig. 3a). During the breeding season, the capsule ($12.23 \pm 9.56\text{mm}^3$) and ingesting ($10.00 \pm 5.81\text{mm}^3$) glands distend to a similar extent, and the ingesting gland gains bright red pigmentation (Fig. 3b). The ingesting gland maintains this enlarged state over the egg-laying ($8.96 \pm 3.20\text{mm}^3$) and post-reproductive ($8.41 \pm 4.80\text{mm}^3$) seasons, and develops a brown appearance (Fig. 3c). In contrast, the capsule gland decreases in volume ($3.02 \pm 1.11\text{mm}^3$) as the reproductive season draws to a close.

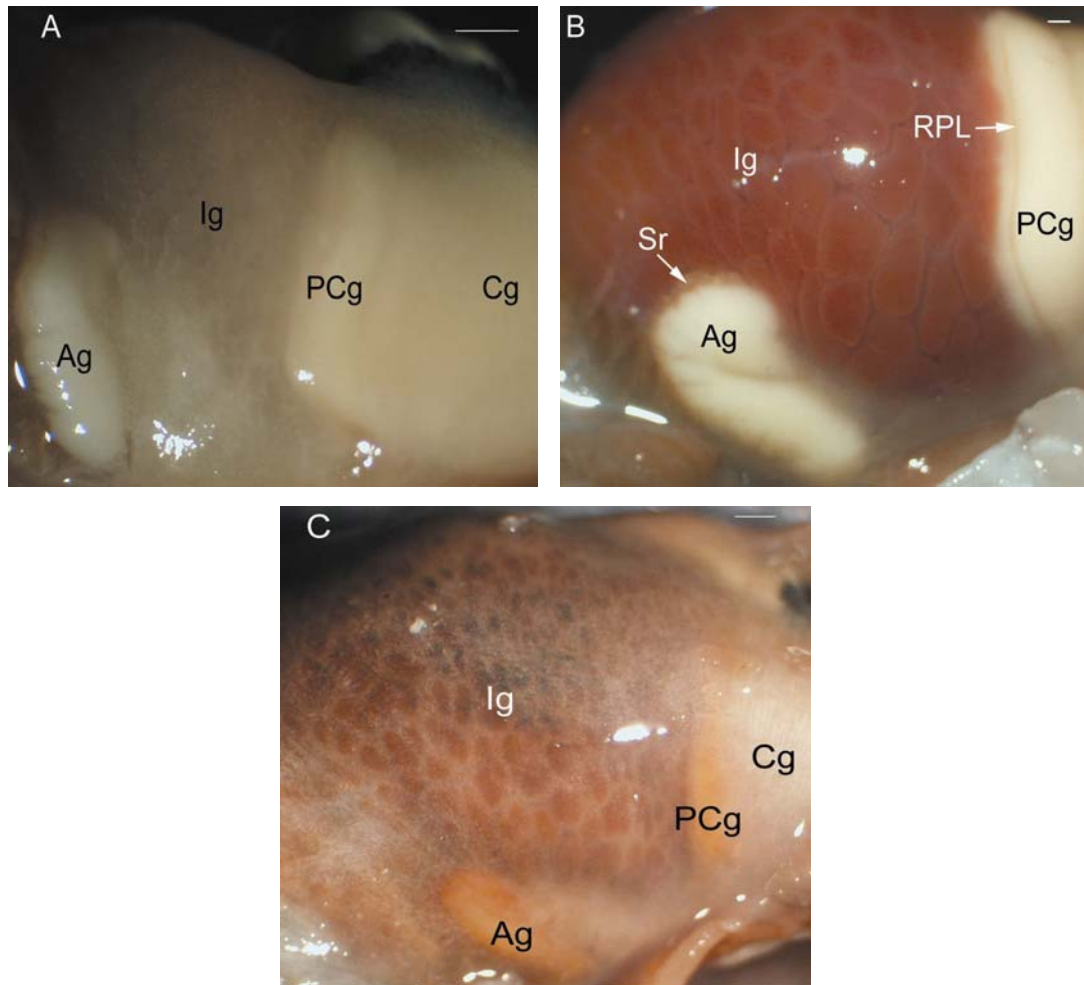


Figure 3. The right side of the posterior pallial gonoduct displaying changes in ingesting gland (Ig) size and pigmentation as a function of reproductive state. The ingesting gland is (A) devoid of pigmentation in pre-reproductive females, (B) bright red and distended in breeding and egg-laying females, and (C) brown in post-reproductive specimens. The albumen gland (Ag) also gains orange pigmentation during this period (C). Cg, capsule gland; PCg, posterior capsule gland lobe; RPL, red pigmented line; Sr, seminal receptacles. Scale bars = 1mm.

3.3.1 Pallial gonoduct histochemistry

The vaginal opening is lined with ciliated columnar epithelial cells interspaced with goblet cells, and is surrounded by a thick layer of smooth circular muscle and an outer layer of longitudinal muscle. Posteriorly, the vaginal opening becomes the ventral channel, developed from a left longitudinal fold in the underlying musculature, which bends back on itself just left of a smaller right longitudinal fold, to form a semi-enclosed duct (Fig. 4a). The cilia are significantly longer (30µm) in this region of the ventral channel, being approximately twice the height of columnar epithelial cells. The ventral channel maintains this morphology as it progresses posteriorly along the pallial gonoduct, ventral to the right capsule gland lobe. Upon reaching the anterior ingesting gland, the left longitudinal fold unites with the ventral musculature creating a functionally closed duct. The columnar epithelium possesses subtle longitudinal folds owing to undulations in the underlying layers of circular and longitudinal muscle and is absent of cilia and goblet cells. Circular muscle fibers, and to a lesser extent, longitudinal fibers, stain metachromatically with Toluidine Blue. The ventral channel then slowly progresses dorsally over the length of the ingesting gland, to open into the albumen gland.

3.3.1.0 The capsule gland

The anterior capsule gland is composed of four distinct lobes; an anteroventral lobe, a small dorsal lobe and left and right lateral lobes (Fig. 4a). A dorsoventral lumen is formed between the lateral lobes (Fig. 4a). The anteroventral lobe appears as a well defined longitudinal glandular fold, originating ventral to the right lateral lobe and extending left over the left longitudinal fold of the ventral channel (Fig. 4a). This

lobe effectively divides the ventral portion of the dorsoventral lumen into transverse lumina, with the right extension being terminal and the left turning back on itself to meet with the ventral channel (Fig. 4a).

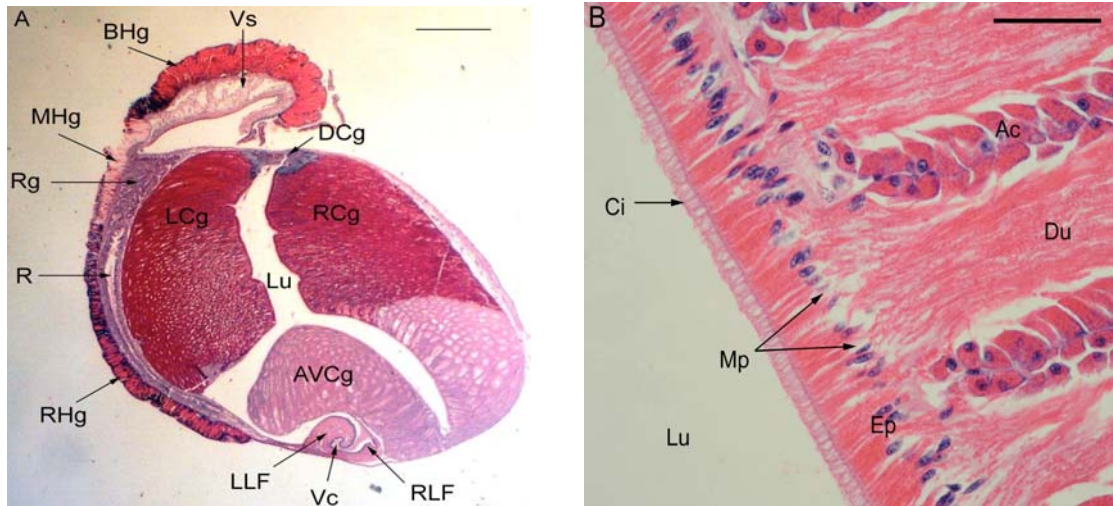


Figure 4. A transverse section through the medial capsule gland stained in H&E showing (A) the lobed configuration of the capsule gland, the anatomical positioning of the hypobranchial gland in relation to the pallial gonoduct and their associated structures; and (B) acinuous cells (Ac) of the anteroventral capsule gland lobe (AVCg) releasing eosinophilic secretory spherules into ducts (Du), which open into the lumen (Lu) through micro-pores (Mp) between ciliated (Ci) epithelial cells (Ep). BHg, branchial hypobranchial gland region; DCg, dorsal capsule gland lobe; LCg, left capsule gland lobe, LLF, left longitudinal fold; MHg, medial hypobranchial gland region; R, rectum; RCg, right capsule gland lobe; Rg, rectal gland; RHg, rectal hypobranchial gland; RLF, right longitudinal fold; Vc, ventral channel; Vs, vascular sinus. Scale bars = 1mm (A) and 50 μ m (B).

The anteroventral lobe is an acinous structure, with subepithelial acini composed of cuboidal cells possessing basal nuclei and prominent nucleoli (Fig. 4b). Acini release a secretory product into numerous ducts, which run parallel to each other and open into the lumen through micro-pores between ciliated columnar epithelial cells (Fig. 4b). The spherical secretion stains lightly eosinophilic, orthochromatic with Toluidine Blue and is positive for Periodic Acid Schiff (PAS). Acini, identical to those of the anteroventral lobe, also comprise the ventral portion of the right lateral lobe (Fig. 4a).

The lateral lobes of the capsule gland are also acinous in arrangement and appear to liberate secretion into the lumen in an identical manner to the anteroventral lobe. The secretion is also packaged in spherules, but is strongly eosinophilic (Fig. 4a), and stains lightly orthochromatic with Toluidine Blue and PAS. The dorsal lobe is composed of comparatively large subepithelial secretory cells, loosely arranged into acini (Fig. 4a). The lobe is penetrated by the dorsal capsule gland lumen, which is lined with ciliated columnar epithelial cells. Dorsal lobe secretory cells release a basophilic (Fig. 4a), weakly PAS-positive amorphous secretion, which stains metachromatic with Toluidine Blue. Secretion within cells of the ventral periphery stains more intensely than that of dorsal acini and appears to be packaged into spherules. In the anterior most region of the capsule gland, these peripheral acini extend ventrally to surround the ventral channel.

The posterior capsule gland is arranged into a right lateral posterior lobe lined anteroventrally with dorsal lobe gland cells and a remnant right lateral lobe (Fig. 5). Just anterior of the posterior lobe, the anteroventral lobe fuses with the ventral region of the right lateral lobe. This effectively terminates the right transverse lumen. The

right lateral lobe then recedes to be replaced by the posterior lobe, which is lined along the left lateral region by gland cells reminiscent of ventral dorsal lobe acini (Fig. 5). Simultaneously, the left lateral lobe is replaced by the left anterior ingesting gland (Fig. 5). This process returns the capsule gland lumen to a dorsoventral slit with a slight right-hand bend into a now open ventral channel (Fig. 5). The posterior lobe is also composed of subepithelial acini, which release a single secretory product into the ventral channel. Secretion spherules originating from these acinous cells stain basophilic, metachromatic purple with Toluidine Blue (Fig. 5), and are strongly PAS-positive.

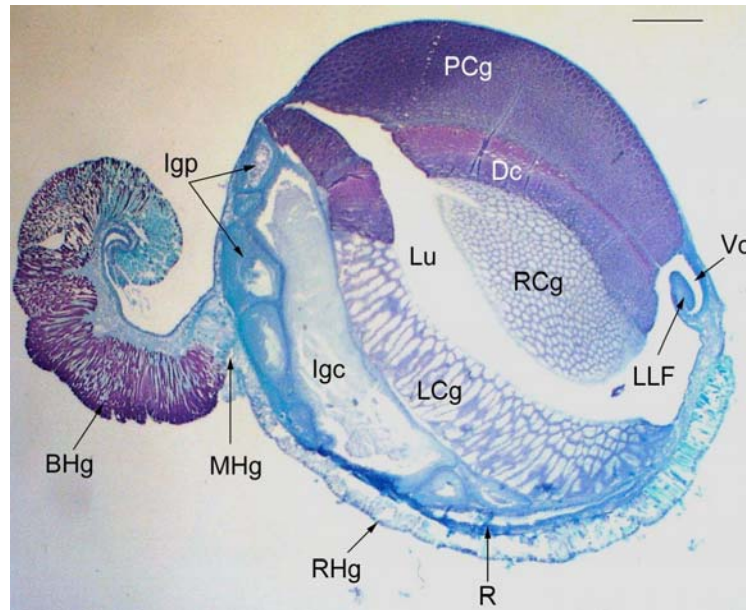


Figure 5. A transverse section through the posterior capsule gland in Toluidine Blue showing the posterior capsule gland lobe (PCg) lined with dorsal lobe cells (Dc) and reduction of the left (LCg) and right (RCg) lobes. The ventral channel (Vc) is open to the lumen (Lu), and the central (Igc) and peripheral (Igp) anterior chambers of the ingesting gland are apparent. BHg, branchial hypobranchial gland region; LLF, left longitudinal fold; MHg, Medial hypobranchial gland region; R, rectum; RHg, rectal hypobranchial gland region. Scale bar = 1mm.

3.3.1.1 The albumen gland

The ovary, which is yellow during the copulatory and egg-laying period, and progressively changes from orange to brown throughout the remainder of the annual cycle, is present on the dorsal surface of the digestive gland (Fig. 1a, 1c). The oviduct proceeds in an anterior direction from the right ventral region of the ovary to open into the lumen of the albumen gland. The albumen gland is composed of left and right lateral lobes joined by a thin suture (Fig. 6a, c), and a dorsoventral lumen lined with ciliated columnar epithelial cells (Fig. 6b). Similar to the capsule gland, subepithelial acini release secretory products into parallel ducts, which open into the lumen through epithelial micro-pores. Two secretory products arise from the albumen gland. The more plentiful amorphous secretion is eosinophilic (Fig. 6a), stains orthochromatically with Toluidine Blue and is PAS positive, while the second is basophilic (Fig. 6a) and stains metachromatic purple with Toluidine Blue. Sperm were observed in the dorsal lumen of one pre-reproductive female and all egg-laying females (Fig. 6b). Of these, two egg-laying females also possessed eosinophilic yolk granules, which stained orthochromatic with Toluidine Blue, and positively with PAS.

Seminal receptacles line the dorsal and posterior periphery of the albumen gland (Fig. 6a, c). Each receptacle opens into the dorsal lumen by means of a short duct, which penetrates the lateral lobe suture. The receptacles are surrounded by a thin layer of smooth circular muscle and subepithelial vascular spaces, supported by loose connective tissue (Fig. 6c). Sperm were commonly observed with their heads buried in the ciliated cuboidal epithelium or as a centrally located mass, embedded in

a PAS-positive material (Fig. 6d). Sperm occupied receptacles of all egg-laying and post-reproductive females and several pre-reproductive and breeding females.

The anterior albumen gland opens into the ventral channel, which is surrounded by a thick layer of smooth circular muscle with longitudinally folded ciliated columnar epithelium, devoid of goblet cells. Sperm were observed with their heads buried in the epithelium of this channel in two copulating and one egg-laying female, which in addition, possessed yolk granules within their albumen glands. The duct leading to the ingesting gland converges with the posterior ventral channel, just anterior of the albumen gland. Similar to the ventral channel, this duct is surrounded by an inner layer of circular muscle, an outer layer of longitudinal muscle and is lined with ciliated columnar epithelium absent of goblet cells (Fig. 7a). Sperm within this duct were positioned as a central mass (Fig. 7a), embedded in PAS-positive secretion. The ingesting gland ducts of all reproductively active females contained sperm (Fig. 7a), with the exception of those containing yolk granules in their albumen glands.

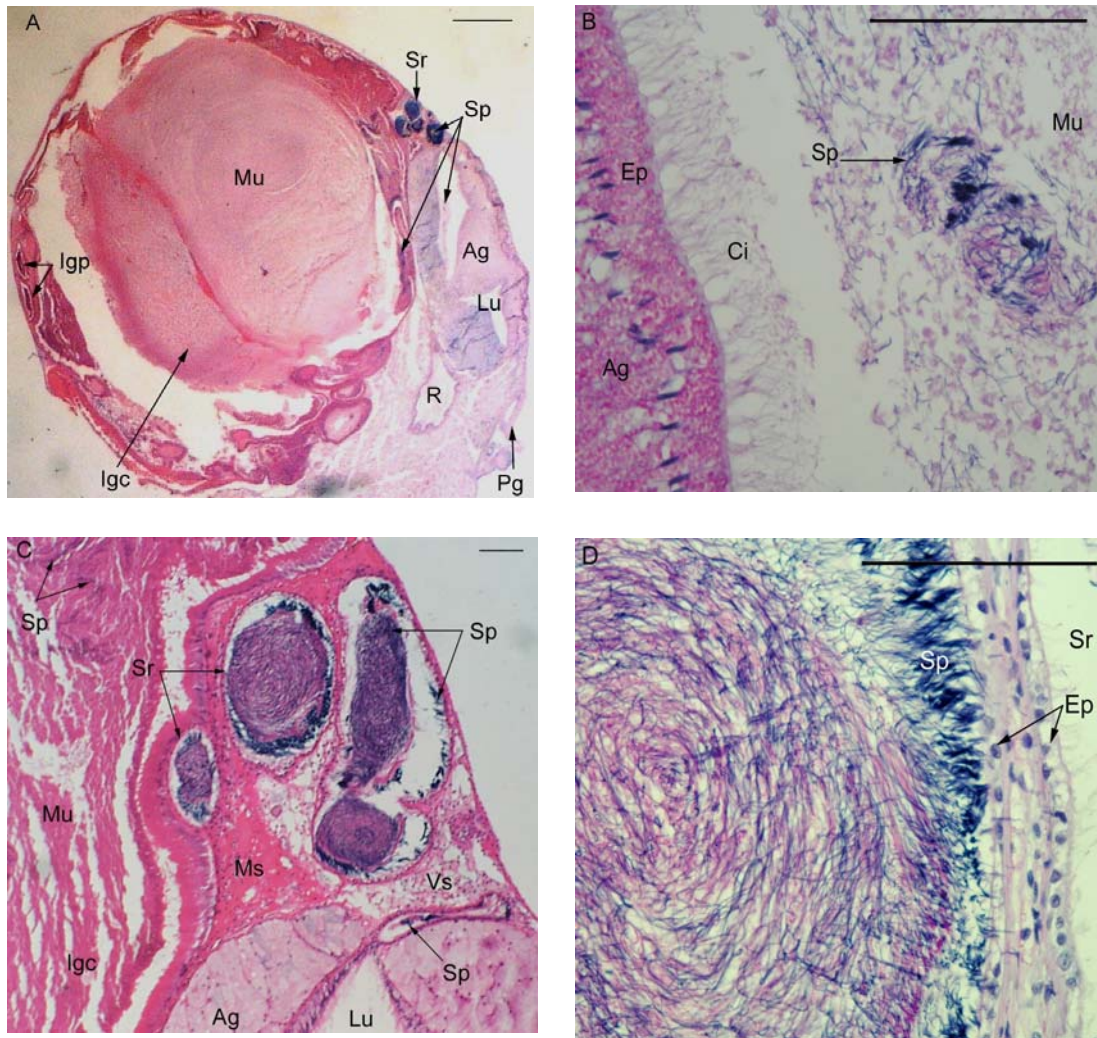


Figure 6. Sperm distribution in the posterior gonoduct of an egg-laying *D. orbita* female. (A) a transverse section through the posterior ingesting gland and albumen gland (Ag) showing the lateral lobes of the albumen gland, seminal receptacles (Sr) and the central (Igc) and peripheral (Igp) ingesting gland chambers in H&E; (B) sperm (Sp) in the dorsal albumen gland lumen (Lu) in PAS positive mucous (Mu); (C) sperm within the seminal receptacles, the central ingesting gland chamber and the duct to the albumen gland stained in H&E; and (D) a seminal receptacle with sperm as a central mass embedded in PAS positive mucous (Mu) and orientated with their heads towards the epithelium (Ep). Ci, cilia; Ms, muscle; Pg, ventral pedal gland; R, rectum; Vs, vascular sinus. Scale bars = 1mm (A) and 100µm (B-D).

3.3.1.2 The ingesting gland

The ingesting gland is composed of a longitudinally folded large central chamber (Fig 7b), which branches off into numerous blind chambers. Each chamber is surrounded by circular muscle (Fig. 7a), which varies substantially in thickness. Transitional epithelium characterizes regions of reduced subepithelial musculature, while polarized columnar cells with microvilli dominate regions overlying thick layers of muscle (Fig. 7a). The latter possess basal nuclei with prominent nucleoli and distinct cytoplasmic domains. The basal domain contains brown elongate endogenous pigments, and eosinophilic spherules which stain orthochromatic with Toluidine Blue. In contrast, spherules in the apical domain stain strongly PAS-positive. Each duct contains masses of secretory material, which appears identical in composition to the apical cytoplasmic domain of columnar epithelial cells (Fig. 7a). Sperm (Fig. 7a) and yolk granules were also embedded in this material, and within the intracellular space of columnar epithelial cells. Sperm were present in the ingesting glands of 75% of females, throughout the annual cycle, while yolk granules were observed in two post-reproductive females.

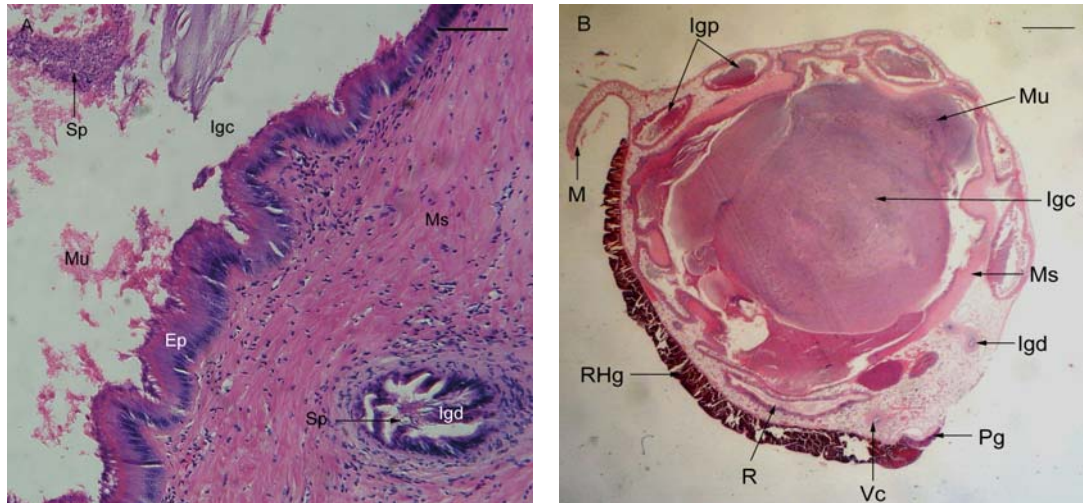


Figure 7. A transverse section through the anterior ingesting gland stained in H&E showing (A) the ingesting gland duct (Igd) with sperm (Sp) as it approaches the central ingesting gland chamber (Igc), which also contains sperm embedded in mucous (Mu); and (B) the central and peripheral (Igp) ingesting gland chambers and the relative position of the ingesting gland duct, ventral channel (Vc) and rectal hypobranchial gland region (RHg). Ep, epithelium; M, mantle; Ms, Muscle; Pg, ventral pedal gland; R, rectum. Scale bars = 50 μ m (A) and 1mm (B).

3. 3. 1. 3 The ventral pedal glands

Two ventral pedal glands are present in female *D. orbita*. The anterior pedal gland commences left of the ventral channel, mid-way along the capsule gland, and appears as a specialized region of ventral mantle epithelium, lining a small protrusion of the subepithelial musculature. The epithelium is composed of ciliated pseudostratified columnar cells, which are narrow at the base, broaden distally and possess elongate apical nuclei. These are interspaced with goblet cells and a second

secretory cell with eosinophilic spherules, which stain orthochromatic with Toluidine Blue.

The posterior ventral pedal gland is more developed than the anterior, and emerges from the ventral mantle as a prominent muscular papilla (Fig. 6a, 7b), which extends along the length of the ingesting gland. The comparatively squat ciliated columnar epithelium is folded longitudinally, and is comprised of numerous goblet cells, interspaced with eosinophilic and basophilic secretory cell types. Eosinophilic cells increase in frequency posteriorly and contain spherules, which stain orthochromatic with Toluidine Blue and are PAS-positive. The basophilic secretory cells also contain spherules, but fail to stain with PAS and Toluidine Blue. In addition to secretion produced by epithelial cells, the posterior ventral pedal gland was observed to receive secretions from rectal hypobranchial gland epithelial cilia in two individuals. Subepithelial gland cells were not observed in association with either pedal gland.

3.3.2 Hypobranchial gland histochemistry

The hypobranchial gland is composed of unusually tall ciliated and non-ciliated pseudostratified columnar epithelial cells (Fig. 8). Based on cell type locality, the branchial and rectal regions can be further subdivided into proximal and distal portions. All regions of the hypobranchial gland are separated from adjacent structures by a continuous vascular sinus, composed of vascular spaces supported by loose connective tissue (Fig. 8a). The basal lamina rests on a thin layer of subepithelial smooth muscle, which extends a short distance between the glandular

folds. At least 7 different secretory cell types along with additional ciliated supportive cells, characterize the hypobranchial epithelium of *D. orbita* (Table 1).

Table 1. The morphological and histochemical properties of cells comprising the hypobranchial epithelium of *D. orbita*. Haem, haematoxylin; Homo, homogeneous; Meta, metachromatic; Ortho, orthochromatic; Sup, supportive cell; -, negative; +, weakly positive; ++, strongly positive.

Type	Cilia	Dimensions \pm S. D. (μm)		Secretion	Haem	Eosin	PAS	Toluidine Blue	
		Height	Width					Ortho	Meta
Sup	Yes	*	*	Homo	-	+	-	+	-
I	No	306.17 \pm 65.21	34.27 \pm 9.78	Spherules	-	++	+	+ / ++	-
II	No	255.55 \pm 79.56	4.3 \pm 1.09	Granules	++	-	-	-	purple (+)
III	No	255.38 \pm 80.66	4.3 \pm 0.88	Granules	-	++	-	+	green (+)
IV	No	183.74 \pm 13.23	*	Spherules	-	++	++	+	-
V	No	194.53 \pm 33.19	18.82 \pm 4.41	Thread-like	+	-	-	-	-
VI	No	201.87 \pm 11.87	15.97 \pm 2.86	Spherules	-	-	-	-	-
VII	No	503.72 \pm 37.27	21.24 \pm 4.45	Amorphous	+	-	+	-	purple (++)

* Mean dimensions were unable to be determined due to constriction by adjacent cells.

Ciliated supportive cells represent the most common cell type, and are located between secretory cells (Fig. 8a-d) throughout all three regions of the hypobranchial gland. These cells possess the morphology of an inverted funnel, which rapidly tapers from the epithelial surface towards the basal lamina. Although the course of these cells can be traced a considerable way into the epithelium, their slender form coupled with the distended nature of adjacent secretory cells, renders it impossible to confirm

a connection with the basement membrane. The apical nucleus is spindle-shaped and the eosinophilic cytoplasm stains orthochromatic with Toluidine Blue.

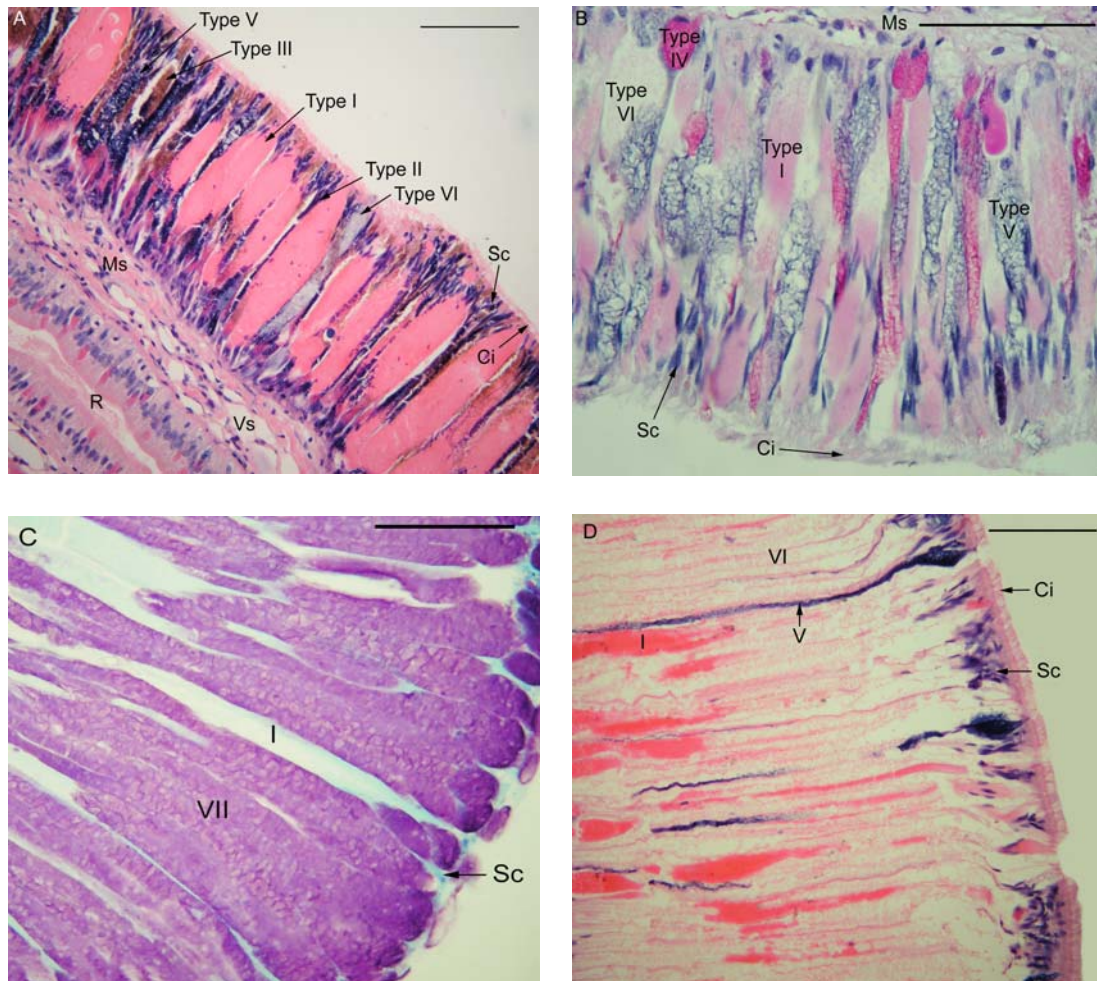


Figure 8. Transverse sections of the hypobranchial epithelium in *D. orbita* showing supportive cells (Sc) and seven secretory cell types. (A) The distal rectal epithelium in H&E, (B) the proximal rectal region in PAS; (C) the proximal branchial epithelium in Toluidine Blue; and (D) the medial region in H&E. Ci, cilia; Ms, muscle; R, rectum; Vs, vascular sinus. Scale bars = 100 μ m.

Type I secretory cells (Fig. 8a-d) are cylindrical in shape, possess round basal nuclei, prominent nucleoli, and are extremely wide (Table 1). These cells dominate

the distal portion of rectal (Fig. 8a) and branchial regions, where they alternate with various combinations of other secretory cells. The frequency of these cells reduces proximally (Fig. 8b-c), although isolated cells remain in the medial region (Fig. 8d). The secretion contains large eosinophilic spherules (Table 1), which appear to partly coalesce in distal lateral cells, but gain separate integrity moving towards the medial region. Toluidine Blue staining intensity from weak to strong (Table 1) correlates with secretion morphology from distal to proximal cells, respectively. Spherules are golden in unstained sections.

Elongate basophilic granules are characteristic of secretory cell type II (Fig. 8a). These cells appear to alternate with cell type I in the distal lateral regions (Fig. 8a) and are also a prominent feature of the proximal portions, but are absent from the medial epithelium. These cells are comparatively slender, devoid of apical cilia (Table 1) and possess round basal nuclei and nucleoli. The secretion is packaged into elongate granules, which appear to maintain this morphology until exocytosed into the mantle cavity. Basophilic granules exhibit weak metachromasia with Toluidine blue (Table 1). Cell type III is commonly paired with type II and likewise, shares a similar distribution (Fig. 8a). Although the morphology of these cells is almost identical, the biochemistry of their secretion granules differs (Table 1). When tightly packed, the apices stain orthochromatic with Toluidine Blue, while loosely packed granules exhibit green metachromasia (Table 1). In the absence of Phloxine B, granules stained eosinophilic (Table 1), while in its presence, granules gained brown-green pigmentation.

Cells reminiscent of goblet cells typify type IV secretory cells (Table 1). These cells possess elongate basal nuclei, distinct nucleoli and are commonly

scattered throughout the proximal lateral regions (Fig. 8b), while isolated cells may also be present in the distal portion and the medial region. Secretory spherules appear to remain membrane-bound until released from the cell. Type V secretory cells contain an unusual basophilic exudate with a thread-like morphology (Table 1). Cylindrical with a dense round nucleus, this cell type appears to in part, replace secretory cell type I in the proximal portion of the rectal (Fig. 8b) and branchial regions of some individuals. Isolated cells also occur in the medial region (Fig. 8d). The medial region of the hypobranchial epithelium is dominated by secretory cell type VI (Fig. 8d), although isolated cells may also occur in the immediately proximal lateral regions. These cells are cylindrical in morphology, comparatively large (Table 1) and possess dense elongate nuclei. Initial observation rendered these cells empty, as the cytoplasm fails to stain with any of the methods applied (Table 1). However, after close examination, large secretory spherules can be seen, faintly outlined by background staining. Secretory cell type VII is also comparatively large (Fig. 8c) with a round basal nucleus and nucleolus. These cells are characterized by an amorphous secretion, which stains strongly metachromatic purple with Toluidine Blue (Table 1). Cells of this type are characteristic of the proximal branchial region (Fig. 8c), although may extend distally in the anterior epithelium of some individuals. Isolated cells were also occasionally observed in the rectal region.

Secretory cell distribution varied considerably among individuals. However, paired cell types II and III were commonly observed to extend from the proximal into the distal portion of both lateral regions. In such individuals, these slender cells alternated with cell type V rather than type I cells. Anteriorly, secretory cells with basophilic amorphous secretion (type VII) appeared to dominate the branchial

epithelium, and in some cases, this dominance was maintained posteriorly. Reproductive state did not appear to affect the chemistry or activity of secretory cells.

3.3.3 Rectal gland and rectum histochemistry

The rectal gland is visible through the dorsal mantle as a dark pigmented anteroposteriorly elongated structure, adjacent to the medial hypobranchial gland (Fig. 1a, c). The anterior rectal gland appears to open into the mantle cavity, while the posterior terminates with the medial hypobranchial gland at the posterior capsule gland (Fig. 1a, c). At no point was the rectal gland observed to connect with the rectum. The rectal gland is acinous in arrangement, with up to 30 acini composed of ciliated cuboidal epithelial cells with dense apical nuclei, and isolated goblet cells (Fig. 9). The subepithelium is devoid of gland cells or musculature, but is rich in vascular spaces supported by loose connective tissue. Dark green-brown pigments ($0.65 \pm 0.07\mu\text{m}$) occupy the cytoplasm of each epithelial cell. Despite their prevalence in the epithelium, these pigments are absent from longitudinal lumina.

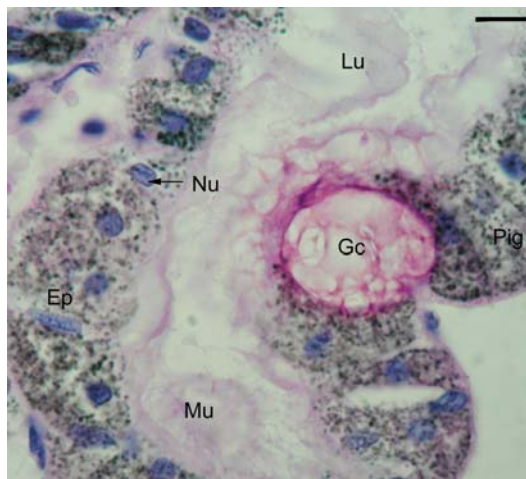


Figure 9. A transverse section through the rectal gland (Rg) stained in PAS showing goblet cells (Gc) and epithelial cells (Ep) containing endogenous pigments (Pig). Lu, lumen; Mu, mucous; Nu, nucleus. Scale bar = 10 μ m.

The rectum commences as a longitudinally folded duct, surrounded by a thin layer of circular muscle, which opens into the mantle cavity via the anus. The rectum is positioned ventral to the rectal gland, left and dorsal to the vaginal opening and is enveloped on its ventral surface by the rectal hypobranchial gland (Fig. 4a). As the anterior capsule gland develops, the rectum elongates dorsoventrally in unison with the left lateral capsule gland lobe and the rectal hypobranchial gland (Fig. 4a). The gland maintains this morphology until the anterior ingesting gland, where the lumen begins to shorten and migrate ventrally (Fig. 5) to finish once again as a longitudinally folded duct, ventral to the ingesting gland (Fig. 6a, 7).

Ciliated pseudostratified columnar epithelial cells line the lumen, which is invariably occupied by waste material. Goblet cells interspaced with secretory cells containing two types of cytoplasmic spherules characterize the rectum epithelium (Fig. 8a). One type is weakly eosinophilic and stains orthochromatically with

Toluidine Blue, while the second is strongly eosinophilic and PAS-positive. In unstained sections, these latter spherules possess golden endogenous pigmentation. Waste material within the lumen stains in an identical manner to the former secretion, although minute endogenous brown pigments may also be present.

3.4 Discussion

3.4.0 Pallial gonoduct functional anatomy

This is the first comprehensive account of the pallial gonoduct and the passage of sperm in *D. orbita* and the subfamily Rapaninae. This process has been described in detail for the Ocenebrinae species, *N. lapillus*, and *O. erinacea* (Fretter, 1941; Tan, 2003), and to some extent in *C. giganteus* (Jaramillo, 1991). Nevertheless, the exact location of fertilization still remains uncertain in the Muricidae, although the lumen of the albumen (Fretter, 1941; Kool, 1988; Jaramillo, 1991) or capsule gland has been proposed (Fretter, 1941). Progressive collection of histomorphological data from females over the reproductive cycle has revealed the course of sperm prior to and post-copulation in *D. orbita*, which strongly suggests that fertilization occurs in the albumen gland lumen. The passage of sperm in *D. orbita* was also found to be more complex than that described for the Ocenebrinae, due to the presence of multiple seminal receptacles (Fig. 6) and a chambered ingesting gland (Fig. 7).

In *D. orbita*, sperm enter the vaginal opening, where they are mixed by ciliary action with mucous secreted by epithelial goblet cells and passed into the semi-enclosed ventral channel. Circular and longitudinal muscle fibers surrounding the ventral channel exhibit metachromasia after Toluidine Blue, indicating the presence

of an actomyocin-like protein for muscle contraction (Szent-Gyorgyi and Kaminer, 1963). The combination of these muscle types produces peristaltic contractions, which drive the mass posteriorly along the ventral channel towards the anterior albumen gland, where the duct to the ingesting gland also intercepts. Once in the posterior ventral channel, sperm may be directed into the dorsal lumen of the albumen gland (Fig. 6a-b) and subsequently the seminal receptacles (Fig 6a, c-d), or the duct to the ingesting gland (Fig. 7a). The entrance to each route is surrounded by thick circular muscle, which suggests females have control over the destination of male gametes by action of a sphincter. Upon entering the dorsal lumen of the albumen gland, sperm are passed into seminal receptacles (Fig 6a, c-d), where they are stored until required for fertilization.

Relaxation of the oviduct sphincter allows oocytes to enter the ventral lumen of the albumen gland, which is formed between left and right lateral lobes. These lobes are acinous in arrangement and release two distinct secretions through micropores in the ciliated columnar epithelium. Biochemical correlations between yolk granules in the dorsal albumen gland lumen and the more abundant albuminous secretion, suggests that this most likely comprises the perivitelline fluid. With the arrival of oocytes, spermatozoa embedded in central mass of glycoprotein-rich mucous are released into the dorsal lumen, presumably by muscular assisted ciliary action of the receptacles. As fertilization should feasibly occur before nutritive and capsule materials are secreted around the eggs, the lumen of the albumen gland has been suggested as the site of fertilization (Kool, 1988). This has also been supported by observations of sperm in the albumen surrounding eggs of *C. giganteus* (Jaramillo, 1991). Alternatively, Fretter (1941) suggested that sperm may be introduced to

oocytes within the capsule gland (Fretter, 1941). In the present study, sperm were exclusively observed within the albumen gland lumen of four females, which strongly implies that this is where fertilization occurs. The apparent restriction of sperm to the dorsal lumen suggests that the secretion of perivitelline fluid is synchronized with fertilization.

Post fertilization, oocytes and albumen may be passed into the ventral channel and driven by muscular assisted ciliary action towards the posterior capsule gland. This mechanism is quite similar to that observed in *O. erinacea*, but different to that of *N. lapillus*, where oocytes enter a separate duct, which opens onto the posterior capsule gland (Fretter, 1941). In the posterior capsule gland of *D. orbita*, the ventral channel is open to the lumen, due to the loss and subsequent reduction of right and left lateral lobes, respectively (Fig. 5). Once within the lumen, capsule gland acini liberate secretion through micro-pores situated between ciliated columnar epithelial cells (Fig. 4b). The secretion is then mixed presumably by ciliary action to form the egg capsule. Only on one previous occasion has a capsule been observed within the pallial gonoduct of a muricid (Fretter, 1941). Although numerous *D. orbita* specimens were examined in the hope of providing another example of capsule formation in the Muricidae, none were present in the egg-laying females dissected. It is likely that the process closely follows that described for *N. lapillus* (Fretter, 1941). However, in the current investigation, the lateral, dorsal and anteroventral lobes produce discrete protein or carbohydrate secretions rather than the mixture of protein and mucoid secretions reported for *N. lapillus*, and instead of posterior lateral tips, *D. orbita* possesses a distinct right posterior lobe (Fig. 5).

The anterior pedal gland in *D. orbita* is composed of specialized mantle epithelium, lining a muscular protrusion ventral and left of the ventral channel, midway along the capsule gland. The posterior ventral pedal gland is more developed and emerges as a prominent muscular papilla in the ventral mantle (Fig. 7b). Both pedal glands possess ciliated columnar epithelium, interspaced with numerous goblet cells and eosinophilic secretory cells, while the posterior pedal gland has in addition, basophilic secretory cells. Although the function of each cell type is unknown, ventral pedal glands are involved in the secretion of an outer capsule layer (Sullivan and Mangel, 1984), capsule shaping and attachment to the substrate (Fretter, 1941). Thus, it seems likely that goblet cells may provide lubrication for capsule shaping by muscular assisted ciliary action, while the remaining secretory cells produce the surface lamina and an adhesive for substrate attachment.

The epithelium of the anterior pedal gland correlates well with that of *O. erinacea*; however the subepithelial morphology of both anterior and posterior ventral pedal glands differs considerably. In *O. erinacea*, clusters of gland cells open into a common lumen below the basal lamina (Fretter, 1941). These features are not present in *D. orbita*, where the secretion is derived exclusively from epithelial cells. Another noticeable difference is in the posture of the posterior gland, which in *O. erinacea* appears as a pit, with a concave anterior and convex posterior (Fretter, 1941), while in *D. orbita* the gland is a shallow convex papilla lying parallel to the ventral mantle. These variations in morphology can be explained by differences in capsule form. In *O. erinacea* the capsule base is shaped like the stem of a wine glass (Hawkins and Hutchinson, 1988), while that of *D. orbita* tapers slightly (D'Asaro, 1991).

Sperm presence within the seminal receptacles of *D. orbita* females from August, 2005 through to July, 2006, suggests that sperm storage for up to ten months may be possible. Sperm may alternatively be replenished through repeat copulations; however the occurrence of such behaviour is unknown for *D. orbita*, which forms annual mating aggregations over spring (Phillips, 1969, Pers. Obs.). Cyclic temperature-dependent spermatogenesis in other temperate muricids together with observed reproductive synchrony between sexes suggests that continuous copulation throughout the year is unlikely (Ramorino, 1975). In the Chilean muricid *C. concholepas*, the onset of vitellogenesis is morphologically characterized by a change in ovary colour from brown to yellow (Ramorino, 1975). As the spawning period ends, the ovary gains orange pigmentation and finally a brown appearance in a pre-vitellogenic state (Ramorino, 1975). Spermatogenesis is closely correlated with oocyte maturation, being heightened during late vitellogenesis, and declining over the spawning season (Ramorino, 1975). When females are in a pre-vitellogenic state, spermatogenesis is greatly reduced and seminiferous tubules are generally absent of sperm (Ramorino, 1975). A similar pattern in ovarian morphology was observed in *D. orbita*, whereby the ovary is yellow during the copulatory and egg-laying period, and progressively changes from orange to brown over the remainder of the annual cycle. Although reproductive synchrony between sexes is yet to be confirmed in *D. orbita*, morphological correlations in the progression of vitellogenesis suggest *D. orbita* and *C. concholepas* adopt similar reproductive strategies. Thus it can be hypothesized that sperm within the seminal receptacles of pre-copulatory and therefore, pre-vitellogenic females, is stored from the previous reproductive phase.

The presence of sperm within seminal receptacles of female *D. orbita* for up to ten months greatly exceeds previous reports for the Muricidae. Sperm have been shown to survive for four months in *C. concholepas* (Ramorino, 1975), and observations of sperm with their heads in the distal epithelium of *C. giganteus* receptacles, suggest they are maintained on nutritive epithelial secretions (Jaramillo, 1991). Sperm were also observed in this orientation in *D. orbita*, although many were embedded in a central mass of glycoprotein-rich mucous (Fig. 6d). The origin of this secretion is unclear, as seminal receptacle epithelium does not appear secretory in nature. However, similarities between the staining reactions of this mucous and the more plentiful albumen gland secretion (Fig. 6b, d), suggest this may be the source.

Storage of viable sperm until the following breeding season has been reported for other gastropods such as the helioid, *Arianta arbustorum* (Chan and Baur, 1993). Sperm storage throughout the annual cycle may reflect a year of inadequate reproductive resources. Alternatively, long-term sperm storage may be an indicator of cryptic female choice. Cryptic female choice is a form of sexual selection, whereby the manipulative processes are confined to the female gonoduct (Bojat et al., 2002). It has been suggested that the complex multi-tubule morphology of the spermatheca in *A. arbustorum* (Baur, 1994; Haase and Baur, 1995) allows female sperm selection. The morphological resemblance of the multiple seminal receptacles of *D. orbita* to those of *A. arbustorum*, suggests they may also function to influence paternity in some Muricidae.

A second indicator of cryptic female choice is the presence of a gametolytic gland. In many pulmonate gastropods, sperm storage is coupled with the presence of a gametolytic gland, which may also aid male gamete selection for fertilization (Lind,

1973; Tompa, 1984; Haase and Baur, 1995). Digestion of surplus sperm occurs in ingesting glands of the Muricidae (Fretter, 1941; Huaquin and Bustos-Obregon, 1981), including *D. orbita* (Fig. 7a). In *D. orbita*, sperm were observed in the duct of the ingesting gland (Fig. 7a) within all reproductively active females, except for those with yolk granules in the albumen gland lumen. The presence of vitelline material indicates that oocytes were near to, or recently released into the albumen gland, which implies that sperm entry into the ingesting gland may only occur prior to or post-fertilization. Consequently, this would ensure fertilized oocytes pass along the ventral channel to the capsule gland, whilst allowing the regulated digestion of surplus sperm within the ingesting gland. Masses of sperm embedded in mucus commonly occupied large central chamber of the ingesting gland (Fig. 7a), while partially digested gametes were observed within the intracellular space of epithelial cells. The ingesting gland of *D. orbita* contained male gametes throughout the copulatory, egg-laying and post-reproductive season. This greatly surpasses previous reports of their presence for one month post-copulation in *C. concholepas* (Huaquin and Bustos-Obregon, 1981). Yolk granules also occupied the central duct and cytoplasmic vacuoles of two post-reproductive *D. orbita* females. This has also been observed in *O. erinacea* (Fretter, 1941) and implies the ingestion of both male and female surplus gametes is possible.

The simultaneous presence of sperm in the ingesting gland and seminal receptacles of *D. orbita* suggests that stored sperm may be directed to the ingesting gland for different purposes. Similar to pulmonates, it appears that sperm are digested in the ingesting gland, possibly for nutritive purposes (Lind, 1973; Birkhead et al., 1993). In contrast, sperm may be directed to the ingesting gland rather than the

seminal receptacles to prevent fertilization by low quality donors (Birkhead et al., 1993) during the copulating period. While either seminal receptacles or an ingesting gland are absent in some muricids, many possess single anterior or multiple posterior receptacles together with an ingesting gland (Kool, 1993; Tan, 2003). Consequently, sexual selection in the form of cryptic female choice may be operating to different degrees with the Muricidae. For instance, species with both these glandular structures would gain maximum individual and offspring fitness benefits, while species with one would be deprived of energy reserves afforded by the digestion of gametes or sperm selection capacity. Overall, this temporal investigation has highlighted the potential for long-term sperm storage and digestion of surplus gametes in *D. orbita*. These findings together with morphological similarities between the receptacles of *D. orbita* and *A. arbustorum*, suggest that *D. orbita* may exercise cryptic female choice to maximize both offspring and individual fitness. However paternity analysis under controlled conditions is required to confirm this.

3. 4. 1 Taxonomic implications

Key morphological attributes of the bursa copulatrix, seminal receptacles, ingesting, capsule and albumen glands have been employed in recent phylogenetic analyses of the Muricidae (Kool, 1993; Tan, 2003). Of the albumen gland morphologies established (Kool, 1993), the juvenile albumen gland of *D. orbita* has been depicted as resembling both omega- and arch-shaped types, while that of adults was difficult to discern. Later, Tan (2003) described the gland as horse-shoe in appearance. The albumen gland in the 12 specimens examined in this investigation appeared as a laterally compressed, sigmoid-shaped structure with 7-8 seminal

receptacles lining the dorsal and posterior periphery (Fig. 1b). This description differs from previous reports of the Rapaninae and suggests that the albumen gland of *D. orbita* is a combination of staff- (e.g. *Morula uva*) and omega-shape (e.g. *Stramonita haemastoma*) types with respect to morphology and seminal receptacle organization, respectively. These observations imply that *D. orbita* displays a convergence in reproductive glandular states known for the Rapaninae, which may ultimately have implications for classifications based on these characters.

Ingesting gland morphology has also served as a trait in taxonomic investigations of the Muricidae, however the seasonal plasticity of this organ has not been considered. The ingesting gland of *D. orbita* has previously been described as a dirty white granular mass, of similar size to the capsule gland (Kool, 1993). The current investigation found this to only be true when the gland is devoid of spermatozoa, usually just prior to the breeding season (Fig. 3a). During the remainder of the annual cycle, the ingesting gland gains bright red (Fig. 3b) and brown pigmentation (Fig. 3c) and attains volumes triple that of the capsule gland in a post-reproductive state due to the insurgence of sperm. Pigment and size plasticity has also been documented for this gland in *C. concholepas* (Ramorino, 1975). Together these findings highlight the need to consider reproductive status when including such character states as a phylobase for the Muricidae.

Among the attributes of the capsule gland, Aungtonya (1997) proposed the ventral channel as a useful diagnostic feature. The ventral channel of *D. orbita* develops between a left longitudinal fold, which bends back on itself, just left of a smaller right longitudinal fold, to form a semi-enclosed duct. This “looped” morphology is similar to that of *N. lapillus* (Fretter, 1941). The channels of *C.*

capucinus and *C. ramosus* (Aungtonya, 1997) were also found to be more similar to *N. lapillus* than *O. erinacea*, which has a third accessory longitudinal fold (Fretter, 1941). These commonalities between the Ocenebrinae (*N. lapillus* and *O. erinacea*), Muricinae (*C. capucinus* and *C. ramosus*) and Rapaninae (*D. orbita*) further contribute to the difficulties in using reproductive morphology to establish the subfamilial placement of species within the Muricidae.

3.4.2 Hypobranchial gland histochemistry

Temporal examination of the hypobranchial gland was conducted to determine if structural or chemical changes occur in synchrony with the reproductive cycle to accommodate the transfer of bioactive Tyrian purple precursors to egg capsules. Despite previous reports of increased secretory activity during the breeding season (Fretter and Graham 1994), reproductive status failed to affect the activity or biochemistry of secretory cells in *D. orbita*. It should be noted that a gross morphological change in pigmentation was observed (Fig 2) that could not be confirmed or explained by histochemical means. Nevertheless, examination of secretory cell biochemistry in conjunction with the pallial gonoduct and associated structures has provided additional information on the comparative function of the hypobranchial gland, Tyrian purple synthesis and precursor transfer.

The anteroposteriorly elongated hypobranchial gland of *D. orbita* is divided into branchial, medial and rectal regions (Fig. 4a). The epithelium is penetrated a short distance by longitudinal folds in subepithelial muscle. Nerve cells were not observed in the hypobranchial gland of *D. orbita*, despite proposed neurological control over secretion release in *N. lapillus* (Bernard, 1890), *Buccinum undatum*

(Hunt, 1973), and *M. granulata* (Srilakshimi, 1991). In *D. orbita*, secretions appear to be released by muscular stimuli, as suggested for *T. haemastoma canaliculata* (Roller et al., 1995). The hypobranchial epithelium of *D. orbita* is characterized by ciliated supportive cells and at least 7 secretory cell types (Table 1).

Ciliated supportive cells arise between groups of secretory cells and are thought to provide support through the formation of intracellular junctions (Hunt, 1973). Similar cells also occur in *B. undatum* (Hunt, 1973), *M. brandaris* (Bolognani-Fantin and Ottoviani, 1981), *M. granulata* (Srilakshimi, 1991), *T. haemastoma canaliculata* (Roller et al., 1995) and various opisthobranchs (Wägele et al., 2006). Although these cells play no apparent role in the secretion process, they may assist in combining secretory products released from adjacent cells, and moving this viscous secretion over the epithelial surface (Hunt, 1973). All secretions from the hypobranchial gland of *D. orbita* remain membrane-bound until exocytosed from the cell where they are directed to the medial depression. In contrast, secretions from the posterior distal rectal region appear to be driven towards the posterior ventral pedal gland. This may facilitate the transfer of hypobranchial secretions to the outer lamina of egg capsules during capsule molding. However, as the outer lamina degrades ≤ 1 wk post deposition (Lim et al., 2007), this mechanism fails to explain the high concentration of Tyrian purple precursors present in capsules during the remainder of the encapsulation period (Benkendorff et al., 2000). Thus, an alternative mode of incorporating bioactive intermediates into egg capsules for larval chemical defence remains to be identified in the Muricidae.

Two secretory cell types appear to occur exclusively within muricid hypobranchial glands, which suggest they may be associated with Tyrian purple production. Cell type I contains large eosinophilic spherules which stain for proteins and carbohydrates (Table 1). Spherules were observed to coalesce in distal cells, but gain separate integrity towards the medial region. Cells displaying a similar shift in secretion morphology have also been reported in the muricid *P. pansa* (Naegel and Aguilar-Cruz, 2006). Secretory cell type VI is characteristic of the medial hypobranchial epithelium of *D. orbita* and is characterized by large secretory spherules, which failed to stain with any of the methods applied (Table 1). These cells may translate to the “empty” or “clear” cells reported in all muricids studied to date (Bolognani-Fantin and Ottaviani, 1981; Srilakshmi, 1991; Roller et al., 1995; Naegel and Aguilar-Cruz, 2006). The absence of these cells from non-muricid species (Tarao, 1935; Ronkin, 1952; Hunt, 1973; Ottaviani, 1978) supports a role in Tyrian purple production. Early investigations of *N. lapillus* (Letellier, 1890; Bernard, 1890) identified cells of the medial zone as “purple-producing”. Later, Erspamer (1946) demonstrated prochromogen presence in the posterior and anterior medial hypobranchial gland of *Murex trunculus* and *M. brandaris*, respectively, while arylsulphatase was limited to the anterior medial region in both species. Thus, it is possible that unstained spherules contain tyrindoxyl sulphate or arylsulphatase. Intracellular localization of these compounds is required to resolve the composition of secretions, and hence confirm the contribution of cell types I and VI to the synthesis of Tyrian purple.

As type I and VI secretory cells appear to be associated with Tyrian purple synthesis in *D. orbita*, sites for precursor transfer to adjacent albumen and capsule

glands may be associated with these cells. The subepithelial space between the hypobranchial gland and the pallial gonoduct is comprised of a continuous vascular sinus. No direct connection was observed between any region of the hypobranchial epithelium and the pallial gonoduct, and examination of secretory cell basal lamina failed to provide evidence for the release of products into subepithelial vascular spaces. The absence of an anatomical means for precursor transfer between the hypobranchial gland and the pallial gonoduct, where precursors have been detected (Westley and Benkendorff, 2008), suggests that these brominated indoles are synthesized within the gonoduct itself. The gonoduct of caenogastropods is thought to have developed from an ancestral right hypobranchial gland (Kay et al., 1998). Consequently, the capacity for Tyrian purple precursor synthesis may have been retained in the reproductive glands of some Muricidae over the course of evolution. This would theoretically facilitate both the synthesis of hypobranchial gland metabolites in the pallial gonoduct and their inclusion in muricid egg masses.

Similarities between the secretory products of hypobranchial gland cells thought to be involved in Tyrian purple synthesis and those of various gonoduct secretions are evident in this investigation. The staining reactions of spherules within hypobranchial gland cell type I correlate with those of the anteroventral and lateral capsule gland lobes and the perivitelline secretion from the albumen gland. Furthermore, the highly sulphated secretion of hypobranchial gland cell type VII is reminiscent of secretions from the dorsal and posterior capsule gland lobes, and the less plentiful albumen gland secretion. As tyrindoxyl sulphate is a sulphate ester of indoxyl (reviewed in Cooksey, 2001a), it is possible that sulphur is sourced from

mucopolysaccharides in both hypobranchial gland cell type VII and the pallial gonoduct.

Although a mode for Tyrian purple precursor transfer was not identified, examination of structures associated with the hypobranchial gland may shed light on the origin of primary metabolites for Tyrian purple synthesis. Dietary derived tryptophan is the most likely origin of the Tyrian purple prochromogen (Westley et al., 2006). The rectum occupies the subepithelial vascular sinus right of the rectal hypobranchial gland and ventral to the rectal gland. Endocytosed eosinophilic spherules in rectum epithelial cells possess golden endogenous pigmentation and stain for mucoproteins. These show remarkable similarity to spherules of type I hypobranchial secretory cells, which suggest that tryptophan may be acquired from waste in the rectum for prochromogen synthesis in the hypobranchial gland. The rectal gland also shares this vascular sinus in the Muricidae (Kool, 1993; Roller et al., 1995; Naegel and Aguilar-Cruz, 2006). This gland functions in the catabolism of haemolymph macromolecules such as tyrosine, which is evidenced by the deposition of melanin in epithelial cells (Andrews, 1992). It is possible that degradation of the tryptophan-containing respiratory pigment, haemocyanin (Waxman, 1975; Avissar et al., 1986) also occurs in rectal epithelial cells. The intimate association between the rectal gland and the medial hypobranchial epithelium where dye secretions accumulate warrants further investigation into the immediate distribution of this amino acid.

Of the secretory cells identified, three new cell types to those previously reported for gastropod hypobranchial glands were observed. Cell type II secretes weakly acidic sulphated mucopolysaccharides, type III contains elongate eosinophilic

granules composed of neutral and phenol-acid mucopolysaccharides, while the biochemical properties of type V remain unclear (Table 1). In contrast, goblet cells rich in glycoprotein (cell type IV) have been reported in neogastropods of the Muricidae (Bolognani-Fantin and Ottaviani, 1981; Srilakshmi, 1991; Roller et al., 1995; Naegel and Aguilar-Cruz, 2006), Buccinidae (Hunt, 1973) and Melongenidae (Ronkin, 1952), basal caenogastropods of the Viviparidae (Ottaviani, 1978) and vetigastropods of the Haliotidae (Tarao, 1935). The wide distribution of these cells throughout Gastropoda reaffirms the primary function of this gland in the production of mucus, to facilitate the binding and removal of particulate matter introduced in the respiratory current (Fretter and Graham 1994). Secretory cells containing highly sulphated mucopolysaccharides (type VII) also appear common to the Neogastropoda (Ronkin, 1952; Hunt, 1973; Srilakshmi, 1991) and shelled opisthobranchs (e.g. Acteonoidea, Cephalaspidea, Sacoglossa and Thecosomata) (Wägele, et al. 2006).

3.5 Conclusion

The current investigation provides the first detailed histological account of the pallial gonoduct and hypobranchial gland of *D. orbita*. This study also expands on previous histomorphological reports of the Muricidae, by simultaneously addressing these glandular regions and associated structures throughout the annual cycle. This approach was primarily adopted to facilitate the identification of an anatomical connection between the gonoduct and hypobranchial gland for the transfer of Tyrian purple precursors to egg masses. Although no obvious mechanism was detected, examination of associated structures has revealed interesting features relevant to the origin of these secondary metabolites. The temporal nature of sampling also allowed

the processes of fertilization to be proposed, a potential capacity for sperm storage and maintenance, and morphological plasticity in the pallial gonoduct of this species. Three additional hypobranchial gland cell types to those reported for other muricids were detected in *D. orbita*, along with another two which may be involved in Tyrian purple synthesis. It is now hypothesized that the prochromogen may be synthesized in the pallial gonoduct. Novel histochemical techniques for the detection of compounds and biosynthetic enzymes required for Tyrian purple genesis have recently been developed to allow further investigation into this proposed source of intermediates in muricid egg masses (Chapters 5 and 6).

3.6 Acknowledgments

I would like to thank, Dr. S. P. Kool, Dr. R. Jaramillo, Dr. P. Middelfart, and Dr. W. F. Ponder for their assistance during early anatomical examinations, and Dr. R. Chase for his insight into pulmonate reproductive strategies. Ms. M. Lewis is also due thanks for providing laboratory space, training in histological techniques and anatomical descriptions, as is Dr. K. Benkendorff for guidance throughout and valuable manuscript feedback. I greatly appreciate the provision of a Flinders University Postgraduate Scholarship. This research was supported by a Philanthropic research grant to Dr. K. Benkendorff.